The Astrophysical Journal, 493:547–554, 1998 February 1

ABSORPTION OF HIGH-ENERGY GAMMA RAYS BY INTERACTIONS WITH EXTRAGALACTIC STARLIGHT PHOTONS AT HIGH REDSHIFTS AND THE HIGH-ENERGY GAMMA-RAY BACKGROUND

M. H. Salamon
Department of Physics, University of Utah, Salt Lake City, UT 84112
and
F. W. Stecker
Laboratory for High-Energy Astrophysics, NASA/Goddard Space Flight Center, Greenbelt, MD 20771
Received 1996 November 20; accepted 1997 September 3

ABSTRACT

In this paper, we extend previous work on the absorption of high-energy γ-rays in intergalactic space by calculating the absorption of 10–500 GeV γ-rays at high redshifts. This calculation requires the determination of the high-redshift evolution of the intergalactic starlight photon field, including its spectral energy distribution out to frequencies beyond the Lyman limit. To estimate this evolution, we have followed a recent analysis by Fall, Charlot, & Pei, which reproduces the redshift dependence of the starlight background emissivity obtained by the Canada-France Redshift Survey group.

We give our results for the γ-ray opacity as a function of redshift out to a redshift of $z = 3$. We also give predicted γ-ray spectra for selected blazars and extend our calculations of the extragalactic γ-ray background from blazars to an energy of 500 GeV with absorption effects included. Our results indicate that the extragalactic γ-ray background spectrum from blazars should steepen significantly above 20 GeV, owing to extragalactic absorption. Future observations of a such a steepening would thus provide a test of the blazar origin hypothesis for the γ-ray background radiation. We also note that our absorption calculations can be used to place limits on the redshifts of γ-ray bursts; for example, our calculated opacities indicate that the 1994 February 17 burst observed by EGRET most probably originated at $z \leq \sim 2$.

Subject headings: diffuse radiation — galaxies: active — galaxies: evolution — gamma rays: bursts — gamma rays: theory

1. INTRODUCTION

The EGRET experiment aboard the *Compton Gamma Ray Observatory* has detected more than 50 blazars extending out to redshifts greater than $z = 2$ (Thompson et al. 1996). It is expected that γ-rays from blazars with energies above the threshold energy for electron-positron pair production will be annihilated through interactions with low-energy intergalactic photons, cutting off the high-energy end of blazar spectra. Such absorption is strongly dependent on the redshift of the source (Stecker, De Jager, & Salamon 1992). Stecker & De Jager (1997) have calculated the absorption of extragalactic γ-rays above 0.3 TeV at redshifts up to 0.54 and presented a comparison with the spectral data for the low-redshift blazar Mrk 421.

The study of blazar spectra at energies below 0.3 TeV is a more complex and physically interesting subject. In addition to intergalactic absorption, one must be able to distinguish and to separate out the effects of intrinsic absorption and natural cutoff energies in blazar emission spectra. Initial estimates of intergalactic absorption of 10 to 300 GeV γ-rays in blazar spectra at higher redshifts have been given by Stecker (1996), Stecker & de Jager (1996), and Madau & Phinney (1996). However, in order to calculate such high-redshift absorption properly, it is necessary to determine the spectral distribution of the intergalactic low-energy photon background radiation as a function of redshift as realistically as possible. This calculation, in turn, requires observation-based information on the evolution of the spectral energy distributions (SEDs) of IR–UV starlight from galaxies, particularly at high redshifts. Conversely, observations of high-energy cutoffs in the γ-ray spectra of blazars as a function of redshift, which may enable one to separate out intergalactic absorption from redshift-independent cutoff effects, could add to our knowledge of galaxy formation and early galaxy evolution. In this regard, it should be noted that the study of blazar spectra in the 10–300 GeV range is one of the primary goals of a next-generation space-based γ-ray telescope, *GLAST* (*Gamma-Ray Large-Area Space Telescope*; Bloom 1996) as well as of a number of ground-based γ-ray telescopes currently under construction.

2. REDSHIFT DEPENDENCE OF THE INTERGALACTIC LOW-ENERGY SED

Our main goal is to calculate the opacity of intergalactic space to high-energy γ-rays as a function of redshift. This depends upon the number density of soft target photons (IR–UV) as a function of redshift, whose production is dominated by stellar emission. To evaluate the SED of the IR–UV intergalactic radiation field, we must integrate the total stellar emissivity over time. This requires an estimate of the dependence of stellar emissivity on redshift. Previous calculations of γ-ray opacity have either assumed that essentially all of the background was in place at high redshifts, corresponding to a burst of star formation at the initial redshift (Stecker 1996; Stecker & De Jager 1996; MacMinn & Primack 1996) or to strong evolution (Madau & Phinney 1996), or that there is no evolution (Madau &

Phinney 1996). In this paper, we use a more realistic model that is consistent with recent observational data on mean stellar emissivity for redshifts $z \leq 1$ (Lilly et al. 1996).

2.1. *Basic Calculation of Stellar Emissivity*

Pei & Fall (1995) have devised a method for calculating stellar emissivity that bypasses the uncertainties associated with estimates of poorly defined luminosity distributions of evolving galaxies. The core idea of their approach is to relate the star formation rate directly to the evolution of the neutral gas density in damped Lyα systems and then to use stellar population synthesis models to estimate the mean comoving stellar emissivity $\mathscr{E}_\nu(z)$ (in ergs s^{-1} cm^3 Hz) of the universe as a function of frequency ν and redshift z (Fall, Charlot, & Pei 1996). Our calculation of stellar emissivity closely follows this elegant analysis, with minor modifications as described below.

Damped Lyα systems are high-redshift clouds of gas whose neutral hydrogen surface density is large enough ($>2 \times 10^{20}$ cm^{-2}) to generate saturated Lyα absorption lines in the spectra of background quasars that happen to lie along and behind common lines of sight to these clouds. These gas systems are believed to be either precursors to galaxies or young galaxies themselves, since their neutral hydrogen (H I) surface densities are comparable to those of spiral galaxies today and their comoving number densities are consistent with those of present-day galaxies (Wolfe 1986). It is in these systems that initial star formation presumably took place, so there is a relationship between the mass content of stars and of gas in these clouds; if there is no infall or outflow of gas in these systems, the systems are "closed," so the formation of stars must be accompanied by a reduction in the neutral gas content. Such a variation in the H I surface densities of Lyα systems with redshift is seen and is used by Pei & Fall (1995) to estimate the mean cosmological rate of star formation back to redshifts as large as $z = 5$.

Pei & Fall (1995) have estimated the neutral (H I plus He I) comoving gas density $\rho_c\,\Omega_g(z)$ in damped Lyα systems from observations of the redshift evolution of these systems by Lanzetta, Wolfe, & Turnshek (1995). (Here $\rho_c = 3H_0^2/8\pi G$ is the critical mass density of the universe. The deceleration parameter is assumed throughout to be $q_0 = 0.5$, with cosmological constant $\Lambda = 0$.) Lanzetta et al. have observed that while the number density of damped Lyα systems appears to be relatively constant over redshift, the fraction of higher density absorption systems within this class of objects decreases steadily with decreasing redshift. They attribute this to a reduction in gas density with time, roughly of the form $\Omega_g(z) = \Omega_{g0}\,e^z$, where $\rho_c\,\Omega_{g0}$ is the current gas density in galaxies. Pei & Fall (1995) have taken selfbiasing effects into account to obtain a corrected value of $\Omega_g(z)$; we have reproduced their calculations to obtain $\Omega_g(z)$ under the assumptions that the asymptotic, high redshift value of the neutral gas mass density is $\Omega_{g,i} = 1.6 \times 10^{-2}\ h_0^{-1}$, where $h_0 \equiv H_0/(100$ km s^{-1} Mpc). In a "closed galaxy" model, the change in comoving stellar mass density $\rho_c\,\dot{\Omega}_s(z) = -\rho_c\,\dot{\Omega}_g(z)$, since the gas mass density $\rho_c\Omega_g(z)$ is being converted into stars. This determines the star formation rate and consequent stellar emissivity (Pei & Fall 1995). The rate of metal production, $\dot{Z}$, is related to the star formation rate by $\Omega_g\,\dot{Z} = \zeta\dot{\Omega}_s$, where $\zeta = 0.38\ Z_\odot$ is the metallicity yield averaged over the initial stellar mass function, with $Z_\odot$ being the solar metallicity (Pei & Fall 1996). This gives a metallicity evolution $Z(z) = -\zeta \ln\,[\Omega_g(z)/\Omega_{g,i}]$.

To determine the mean stellar emissivity from the star formation rate, an initial mass function (IMF) $\phi(M)$ must be assumed for the distribution of stellar masses M in a freshly synthesized stellar population. To further specify the luminosities of these stars as a function of mass M and age T, Fall et al. (1996) use the Bruzual-Charlot (BC) population synthesis models for the spectral evolution of stellar populations (Bruzual & Charlot 1993; Charlot & Bruzual 1991). In these population synthesis models, the specific luminosity $L_{\rm star}(\nu, M, T)$ (in ergs s^{-1} Hz^{-1}) of a star of mass M and age T is integrated over a specified IMF to obtain a total specific luminosity $S_\nu(T)$ per unit mass (ergs s^{-1} Hz^{-1} g^{-1}) for an entire population, in which all stellar members are produced simultaneously ($T = 0$). Following Fall et al. (1996), we have used in our calculations the BC model corresponding to a Salpeter IMF, $\phi(M)\ dM \propto M^{-2.35}\ dM$, where $0.1\ M_\odot < M < 125\ M_\odot$.

The mean comoving emissivity $\mathscr{E}_\nu(t)$ is then obtained by convolving over time t the specific luminosity S_ν with the mean comoving mass rate of star formation, $\rho_c\,\dot{\Omega}_*$:

$$\mathscr{E}_\nu(t) = \rho_c \int_0^t dt' S_\nu(T = t - t')\dot{\Omega}_*(t')\ . \qquad (1)$$

Note that the star mass formation rate $\rho_c\,\dot{\Omega}_*(t)$ that appears in this equation is not the same as $\rho_c\,\dot{\Omega}_s(t)$, the change in total stellar mass density. This is because $\rho_c\,\dot{\Omega}_s$ is the rate at which mass is *permanently* being converted into stars; since some stellar mass is continuously being returned to the interstellar medium (ISM), the *instantaneous* mass rate of star formation $\rho_c\,\dot{\Omega}_*$ is larger than $\rho_c\,\dot{\Omega}_s$, the two being related by

$$\dot{\Omega}_s(t) = \dot{\Omega}_*(t) - \int_0^t dt'\dot{R}(t - t')\dot{\Omega}_*(t')\ , \qquad (2)$$

where $R(T)$, provided by the BC models, is the fraction of the initial mass of a generation of stars formed at $T = 0$ that has been returned to the ISM.

2.2. *Metallicity Corrections*

The BC models' specific luminosities $S_\nu(T)$ are calculated assuming that the metallicity content Z during star formation is fixed at our current solar metallicity value ($Z_\odot = 0.0169$). However, the metallicity content of the universe is not static but, instead, evolves with redshift as early populations of stars return freshly synthesized metals to the interstellar medium during their various phases of mass loss. For example, in a survey of one-third of the known damped Lyα absorbers, Pettini et al. (1994) found that the typical metallicity is 0.1 that of the present solar value at a redshift of $z \approx 2$. Since the specific luminosity of a star of a given mass is also a function of its metallicity content (lower metallicities give bluer spectra), the metallicity of a stellar population must be taken into account when integrating the mean emissivity over redshift.

The effect of metallicity content in stellar population models has been examined by Worthey (1994). Using the IMF $\phi(M)dM \propto M^{-2.35}\ dM$ with $0.1\ M_\odot < M < 2\ M_\odot$, Worthey has calculated the mass-to-light ratios $\langle M/L \rangle$ as a function of population age T and metallicity Z for the color bands U through M. We have plotted his $\langle M/L \rangle$ tabulated values for the B and U bands in Figures 1 and 2, respec-

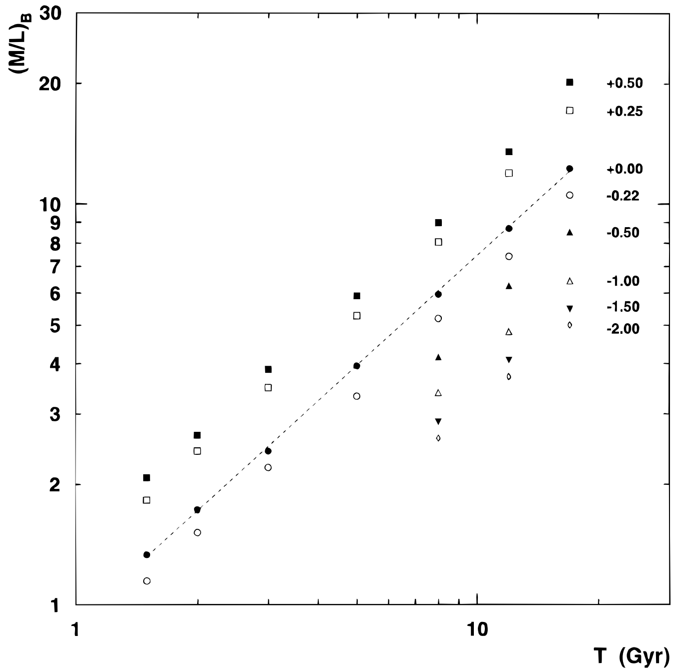

FIG. 1.—Plot of B-band mass-to-light ratios M/L vs. stellar system age T for various values of metallicity Z, taken from Table 5A of Worthey (1994). The metallicity values are given on the right-hand side of the figure as $y \equiv \log (Z/Z_\odot)$, where $Z_\odot$ is solar metallicity. Filled (open) squares correspond to the tabulated data for $y = +0.5$ ($y = +0.25$), filled (open) circles for $y = 0.0$ ($y = -0.22$), filled (open) triangles for $y = -0.5$ ($y = -1.0$), filled inverted triangles for $y = -1.5$, and open diamonds for $y = -2.0$. A straight dashed line has been drawn through the $Z = Z_\odot$ values; at a fixed population age T, the metallicity correction factor for metallicity Z is the vertical displacement from this line to the $Z \neq Z_\odot$ value.

tively. One can see that for a fixed metallicity, the logarithm of the luminosity L decreases nearly linearly with the logarithm of population age T. Also one sees that for a fixed

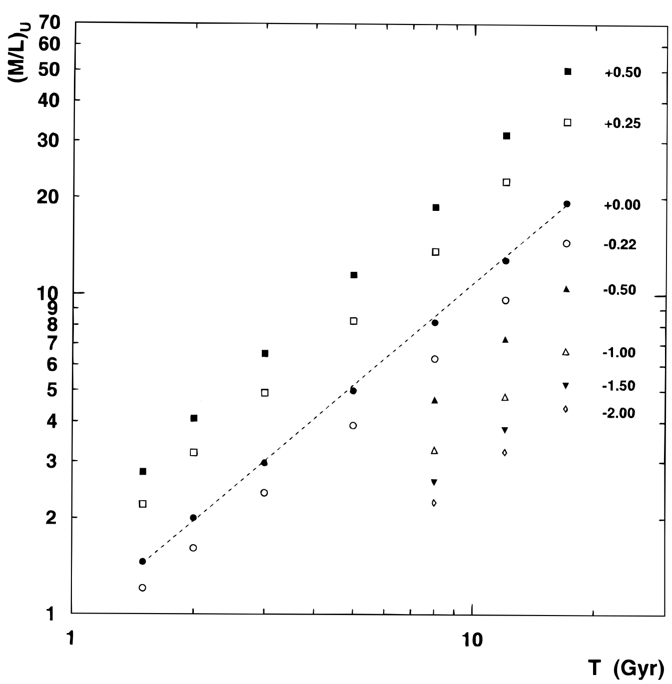

FIG. 2.—Plot of the U-band mass-to-light ratios M/L versus stellar system age T for various values of metallicity Z. See the legend to Fig. 1 for details.

age T, the luminosity $L_{B(U)}$ of the $B(U)$ band decreases, by a factor that is nearly independent of T, as the metallicity increases. This enables us to construct a correction factor $\mathscr{L}_X(Z/Z_\odot) \equiv L_X(Z, T)/L_X(Z_\odot, T)$ for each color band X, which is independent of T, and which gives the logarithmic shift in L_X as one goes from the present metallicity $Z_\odot$ to a different value of Z.

Having obtained correction factors $\mathscr{L}_X(Z/Z_\odot)$ for the $X = U$, B, I, and K bands using Worthey's tabulated $\langle M/L \rangle_X(Z, T)$ values (I- and K-band data are not shown), we find a single "metallicity correction function" $\mathscr{L}(\lambda, Z)$ that interpolates in wavelength λ between each of the individual color band correction factors $\mathscr{L}_X$:

$$\log \mathscr{L}(\lambda, Z) \equiv \log \left[\frac{L(\lambda, Z)}{L(\lambda, Z_\odot)}\right] \approx \left[0.33 - \frac{0.30}{\lambda}\right] \log \left(\frac{Z}{Z_\odot}\right) + \left(0.066 - \frac{0.063}{\lambda}\right)\left[\log \left(\frac{Z}{Z_\odot}\right)\right]^2 \quad (3)$$

This interpolative function is valid only for 0.3 μm $< \lambda <$ 2.2 μm. Outside of this wavelength region, we take $\mathscr{L}(\lambda < 0.3\ \mu\mathrm{m}, Z) = \mathscr{L}(\lambda = 0.3\ \mu\mathrm{m}, Z)$ and $\mathscr{L}(\lambda > 2.2\ \mu\mathrm{m}, Z) = \mathscr{L}(\lambda = 2.2\ \mu\mathrm{m}, Z)$. Note that increased metallicity gives a redder population spectrum (Bertelli et al. 1994).

Limitations to this correction function include the facts that Worthey's calculations apply only to stars with ages greater than $T = 1.5$ Gyr and that the upper mass limit of his IMF (2 $M_\odot$) is much lower than that of the BC model that we employ (125 $M_\odot$). This may be a source of overestimation of the UV radiation density if the higher mass stars have a smaller UV luminosity dependence on metallicity. That this may indeed be the case is suggested by recent calculations of Charlot (Y. Pei & M. Fall 1997, private communication). Population synthesis models in which varying metallicity is included do exist (Bertelli et al. 1994), and efforts to reconcile differences in computed spectra generated by these various models have been made (Charlot, Worthey, & Bressan 1996). An additional uncertainty exists below 0.3 μm, since Worthey's calculations extend only to the U band. We have chosen to assume a constant enhancement factor below $\lambda = 0.3$ μm. For the above reasons, the metallicity correction function given in equation (3) should be regarded as a "maximum" correction, with the true correction factor lying somewhere between equation (3) and $\mathscr{L}(Z) \equiv 1$.

2.3. *Absorption by Dust and Gas within the Source*

The emissivity $\mathscr{E}_\nu$ given in equation (1) assumes that all stellar emission escapes from the gas system that contains the stars. However, some absorption of stellar radiation by both dust and gas occurs within the larger damped Lyα systems. Above the Lyman limit, this absorption is dominated by dust, while below the Lyman limit, absorption by neutral hydrogen and singly ionized helium dominates. Defining the mean transmission fractions, averaged over the optical depths of damped Lyα systems, by $\mathscr{T}_{\mathrm{dust}}(\nu, z)$ and $\mathscr{T}_{\mathrm{gas}}(\nu, z)$, the final expression for the effective stellar emissivity is

$$\mathscr{E}_\nu(z) = \mathscr{T}_{\mathrm{dust}}(\nu, z)\mathscr{T}_{\mathrm{gas}}(\nu, z)\rho_c \int_z^{z_{\max}} \frac{dz'}{H_0(1+z')^{2.5}} \times \dot{\Omega}_*(z')\mathscr{L}[\nu, Z(z')]S_\nu[T = t(z) - t(z')] . \quad (4)$$

The distribution of optical depths τ_d of Lyα clouds caused by dust can be adequately represented by $f(x) = f_0\, x^{-\alpha} e^{-x}$, where $x = \tau_d/\tau_c(z)$, $\tau_c(z)$ being a characteristic (redshift-dependent) cloud dust opacity, and $\alpha \approx 1$ (Fall et al. 1996). Under the assumption that both dust and stars are uniformly distributed throughout each Lyα cloud, the fraction of radiation $\mathscr{T}^{(1)}(\tau_d)$ produced by stars in a given cloud of optical depth τ_d that escapes dust absorption is given by

$$\mathscr{T}^{(1)}(\tau) = \frac{2}{\tau\eta}\left[\frac{1 - e^{-\tau\eta}}{(1 + \eta) + (1 - \eta)e^{-\tau\eta}}\right], \qquad (5)$$

where $\eta = (1 - \omega)^{1/2}$, and ω is the average albedo of dust, taken to be the same as in our Galaxy ($\omega \sim 0.4$–0.6; Whittet 1992). (We have calculated eq. (5) using the two-stream approximation; Chandrasekhar 1950). We note that the dust opacity τ_d in equation (5) is assumed to be proportional to the H I surface column density $N_{\rm H\,I}$ and metallicity Z,

$$\tau_d(\nu, z) = \frac{Z(z)}{Z_\odot}\left(\frac{N_{\rm H\,I}}{6.3 \times 10^{21}\ {\rm cm}^{-2}}\right)E(\nu)\ , \qquad (6)$$

where $E(\nu)$ is the normalized galactic interstellar dust extinction curve (Savage & Mathis 1979). Integrating equation (5) over the Lyα opacity distribution function f of Pei & Fall (1995), we obtain $\mathscr{T}_{\rm dust}(\nu, z)$ and find it to have a minor effect on the emissivity, $\mathscr{T}_{\rm dust}(\nu, z)$ being typically of order unity.

Below the Lyman limit ($\lambda < 0.0912\ \mu$m), the opacity is dominated by neutral gas absorption: $\tau_g(\nu) = N_{\rm H\,I}\sigma_{\rm H\,I}(\nu) + N_{\rm He\,I}\sigma_{\rm He\,I}(\nu)$, where $\sigma_{\rm H\,I}$ and $\sigma_{\rm He\,I}$ are the H I and He I photoionization cross sections. With the $N_{\rm H\,I}$ and $N_{\rm He\,I}$ distributions of the Lyα systems being related to the dust opacity distribution $f(\tau_d)$ through equation (6), the distribution for τ_g can be obtained. Integrating equation (5) (now with $\eta = 1$), weighted with the τ_g distribution, gives $\mathscr{T}_{\rm gas}(\nu, z)$.

2.4. *Numerical Results*

Figure 3 shows the calculated stellar emissivity as a function of redshift at 0.28 μm, 0.44 μm, and 1.00 μm, both with and without the metallicity correction function $\mathscr{L}(\lambda, Z)$. We have also plotted the observations of the cosmic emissivity by the Canada-France Redshift Survey (Lilly et al. 1996) at these rest-frame wavelengths for comparison. With a lower mass cutoff of 0.1 $M_\odot$ in the IMF, we obtain emissivities that are roughly a factor of 2 higher than those obtained by Lilly et al. (1996). To bring our emissivities down to the observed values requires that we reduce the lower mass limit in the IMF to 0.02 $M_\odot$, which puts a fraction (0.45) of the mass into effectively nonluminous compact objects. We note that a similar reduction was achieved by Fall et al. (1996) by modifying the power-law index in the IMF; a higher index results in a lower emissivity (Y. C. Pei 1996, personal communication).

Overall, our emissivities, both with and without the metallicity corrections, are in reasonable agreement with the data at lower redshifts (Lilly et al. 1996). Although the differences for $\mathscr{E}_\nu$ between the no-metallicity and metallicity cases for $z < 1$ are not great, *they become substantial at larger redshifts for both optical and UV wavelengths*. This has notable effects on the opacity of the radiation background to high-energy γ-rays, as will be seen in § 4. We note that our dotted-line curves in Figure 3 (with no metallicity correction) are essentially reproductions of the emissivities calculated by Fall et al. (1996).

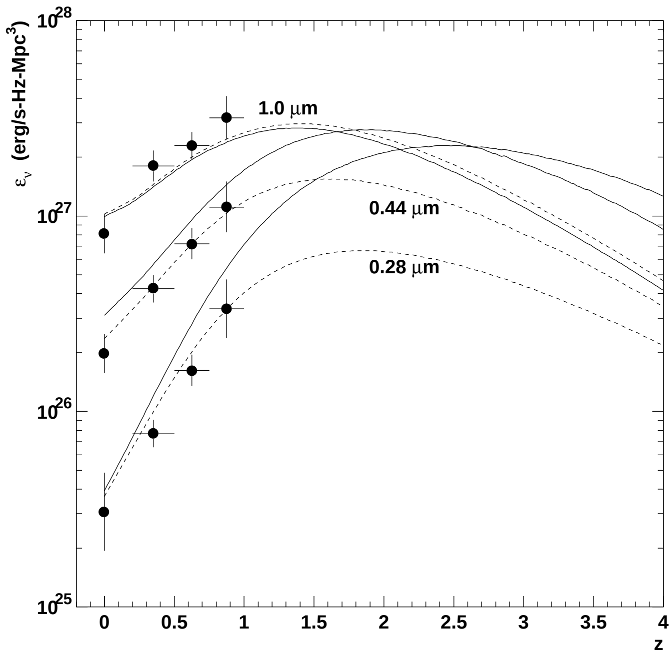

FIG. 3.—Comoving emissivity as a function of redshift, calculated using eq. (4), for three wavelength values, $\lambda = 0.28, 0.44$, and 1.0 μm, for a Hubble constant value of $h_0 = 0.5$. Note that the emissivity scales as h_0^2 (see eq. [4] and § 3). Solid line curves are for the case where the metallicity correction function ($\mathscr{L}$ from eq. [3]) is used. Dashed lines give the emissivity when this correction function is *not* included. The data from the Canada-France Redshift Survey (Lilly et al. 1996) are also plotted.

In all cases as shown in Figure 3, the stellar emissivity in the universe peaks at $1 \le z \le 2$, dropping off at both lower and higher redshifts. Indeed, Madau et al. (1996) have used observational data from the Hubble Deep Field to show that metal production has a similar redshift distribution, such production being a direct measure of the star formation rate. (See also the review by Madau 1997.)

2.5. *Calculation of the Diffuse Radiation Energy Density*

The comoving radiation energy density $u_\nu(z)$ (in ergs cm^3 Hz) is the time integral of the comoving emissivity $\mathscr{E}_\nu(z)$,

$$u_\nu(z) = \int_z^{z_{\rm max}} dz' \mathscr{E}_{\nu'}(z')\, \frac{dt}{dz}\,(z') e^{-\tau_{\rm eff}(\nu, z, z')}\ , \qquad (7)$$

where $\nu' = \nu(1 + z')/(1 + z)$, and $z_{\rm max}$ is the redshift corresponding to initial galaxy formation. The extinction term $e^{-\tau_{\rm eff}}$ accounts for the absorption of ionizing photons by the clumpy intergalactic medium (IGM) that lies between the source and the observer; although the IGM is effectively transparent to nonionizing photons, the absorption of photons by H I, He I, and He II can be considerable (Madau 1995). The presence of damped Lyα and Lyman-limit systems (Lanzetta et al. 1995) and the Lyα forest, coupled with the absence of an H I Gunn-Peterson effect (Gunn & Peterson 1965; Steidel & Sargent 1987) indicates that essentially all of the H I, He I, and He II exists within intergalactic clouds whose measured H I column densities range from approximately 10^{13} to 10^{22} cm^{-2}.

The effective optical depth $\tau_{\rm eff}$ between a source at redshift z' and an observer at redshift z owing to Poisson-distributed intervening Lyα clouds is given by (Paresce,

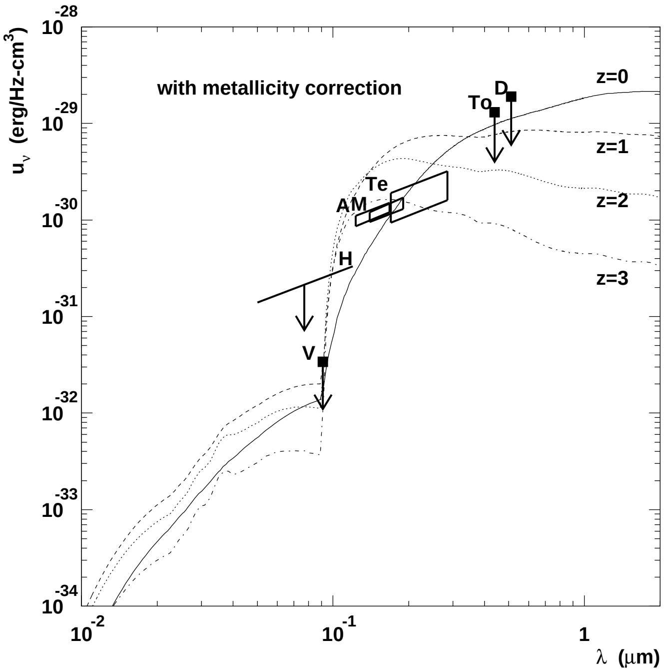

FIG. 4.—Intergalactic comoving radiation energy density from stars, calculated with the metallicity correction function $\mathscr{L}$ included, as a function of wavelength for redshifts $z = 0$ (*solid line*), $z = 1$ (*dashed line*), $z = 2$ (*dotted line*), and $z = 3$ (*dot-dashed line*), for a Hubble constant value of $h_0 = 0.5$. (The energy density scales as h_0; see eq. [7] and § 3.) QSO contributions to the UV energy density have a negligible effect on extragalactic gamma-ray absorption, and so are neglected in our calculations. Also shown in the figure are the high-latitude measurements of Anderson et al. 1979 ("A"), Tennyson et al. 1988 ("Te"), and Martin, Hurwitz, & Bowyer 1991 ("M"), and upper limits from Vogel et al. 1995 ("V"), Toller 1983 ("To"), Dube, Wickes, & Wilkinson 1979 ("D"), and Holberg 1986 ("H"). These data should be compared with only the $z = 0$ (*solid line*) curve.

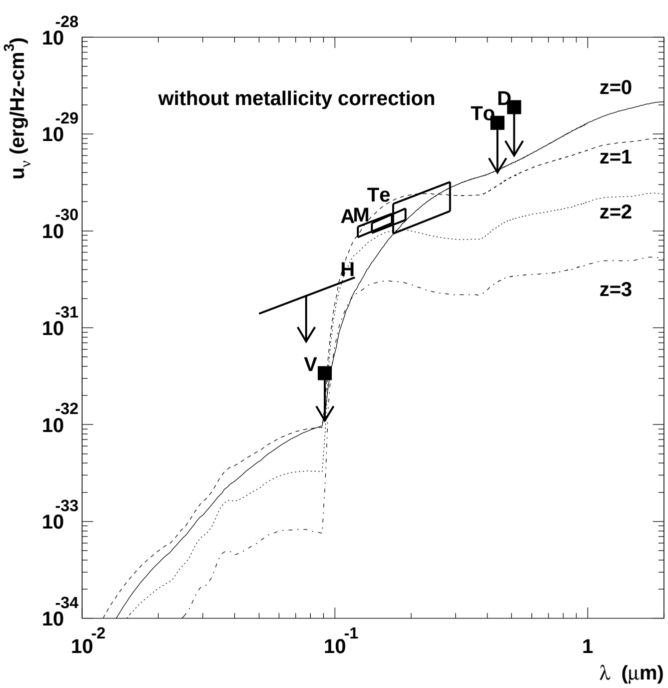

FIG. 5.—Same as Fig. 4 except *without* the metallicity correction function ($\mathscr{L} \equiv 1$ for the energy densities shown here).

McKee, & Bowyer 1980)

$$\tau_{\rm eff}(\nu, z, z') = \int_z^{z'} dz'' \int_0^\infty dN_{\rm H\,I} \frac{\partial^2 N}{\partial N_{\rm H\,I} \partial z''} (1 - e^{\tau(\nu'')}) , \quad (8)$$

where $\tau(\nu) = [N_{\rm H\,I}\sigma_{\rm H\,I}(\nu) + N_{\rm He\,I}\sigma_{\rm He\,I}(\nu) + N_{\rm He\,II}\sigma_{\rm He\,II}(\nu)]$, $\nu'' = \nu(1 + z)/(1 + z'')$, and $\partial^2 N/(\partial N_{\rm H\,I} \partial z)$ is the distribution function of clouds in redshift z and column density $N_{\rm H\,I}$. As pointed out by Madau & Shull (1996), when $\tau \ll 1$, $\tau_{\rm eff}$ is just the mean optical depth of the clouds; when $\tau \gg 1$, $\tau_{\rm eff}$ becomes the number of optically thick clouds between the source and the observer, so that the Poisson probability of encountering no thick clouds is $e^{-\tau_{\rm eff}}$, as required.

For the distribution function of Lyα clouds, we use the parameterization of Madau (1995; see also model A2 of Miralda-Escudé & Ostriker 1990),

$$\frac{\partial^2 N}{\partial N_{\rm H\,I}\, \partial z} = \begin{cases} 2.4 \times 10^7 N_{\rm H\,I}^{-1.5}(1 + z)^{2.46} \\ \qquad 2 \times 10^{12} < N_{\rm H\,I} < 1.59 \times 10^{17}\ {\rm cm}^2 \\ 1.9 \times 10^8 N_{\rm H\,I}^{-1.5}(1 + z)^{0.68} \\ \qquad 1.59 \times 10^{17} < N_{\rm H\,I} < 10^{20}\ {\rm cm}^{-2} . \end{cases} \quad (9)$$

Using equations (8) and (9) and the stellar emissivity $\mathscr{E}_\nu(z)$ in equation (7), we obtain the background energy density $u_\nu(z)$ shown in Figures 4 and 5, calculated with and without the metallicity correction, $\mathscr{L}$, respectively.

Although it is possible that UV emission from QSOs alone may be able to account for the nearly complete reionization of the IGM (Meiksin & Madau 1993; Fall & Pei 1993; Madau & Meiksin 1994), it has been argued that additional sources of ionizing radiation are required (Miralda-Escudé & Ostriker 1990), these perhaps being young galaxies that leak a fraction (up to $\sim$15%) of their ionizing radiation through H II "chimneys" (Dove & Shull 1994; Madau & Shull 1996). We note, however, that recent observations of four starburst galaxies by the Hopkins UV Telescope (Leitherer et al. 1995) indicate that less than 3% of Lyman continuum photons escape from these sources. We have assumed in our calculations that 5% of the stellar emission escapes from the galaxies (protogalaxies) through these chimneys unattenuated by dust or gas.

We have also done these calculations assuming a 15% chimney escape factor and find that the resulting ionizing flux at $z = 0$ is slightly above the upper limit given by Vogel et al. (1995). We also find that changing the chimney escape factor has a negligible effect on our calculated opacities. We conclude that any ionizing flux component consistent with the upper limit of Vogel et al. (1995) is too small to have a significant effect on the γ-ray opacity. For this reason, we do not include a component of ionizing radiation from quasars (see, e.g., Madau 1992) in our opacity calculations.

We also show in Figures 4 and 5 the recent upper limits on the background radiation. It should be noted that our results as shown give emissivities *from starlight only* and do not include dust emissivities in the mid- and far-infrared.

3. OPACITY OF THE RADIATION BACKGROUND AND ITS EFFECT ON BLAZAR SPECTRA

With the comoving energy density $u_\nu(z)$ evaluated, the optical depth for γ-rays owing to electron-positron pair production interactions with photons of the stellar radiation background can be determined from the expression (Stecker et al. 1992)

$$\tau(E_0, z_e) = c \int_0^{z_e} dz \frac{dt}{dz} \int_0^2 dx \frac{x}{2} \int_0^\infty d\nu (1+z)^3 \left[\frac{u_\nu(z)}{h\nu}\right] \sigma_{\gamma\gamma}[s = 2E_0 h\nu x(1+z)] \, , \quad (10)$$

where E_0 is the observed γ-ray energy at redshift zero, ν is the frequency at redshift z, z_e is the redshift of the γ-ray source, $x = (1 - \cos\theta)$, θ being the angle between the γ-ray and the soft background photon, h is Planck's constant, and the pair production cross section $\sigma_{\gamma\gamma}$ is zero for center-of-mass energy $s^{1/2} < 2m_e c^2$, m_e being the electron mass. Above this threshold,

$$\sigma_{\gamma\gamma}(s) = \frac{3}{16}\sigma_T(1-\beta^2)\left[2\beta(\beta^2-2) + (3-\beta^4)\ln\left(\frac{1+\beta}{1-\beta}\right)\right] , \quad (11)$$

where $\beta = (1 - 4m_e^2 c^4/s)^{1/2}$.

Figures 6 and 7 show the opacity $\tau(E_0, z)$ for the energy range 10–500 GeV calculated with and without the metallicity correction. Extinction of γ-rays is negligible below 10 GeV. Above 500 GeV, interactions with photons with wavelengths of tens of μm become important, so one must include interactions from infrared photons generated by dust reradiation (Stecker & De Jager 1997), which we have neglected here. For 300 GeV γ-rays at redshifts below 0.5, our opacities agree with the with the opacities obtained by Stecker & De Jager (1997).

Note that these calculated opacities are *independent* of the value chosen for h_0, as seen in equations (4), (7), and (10).

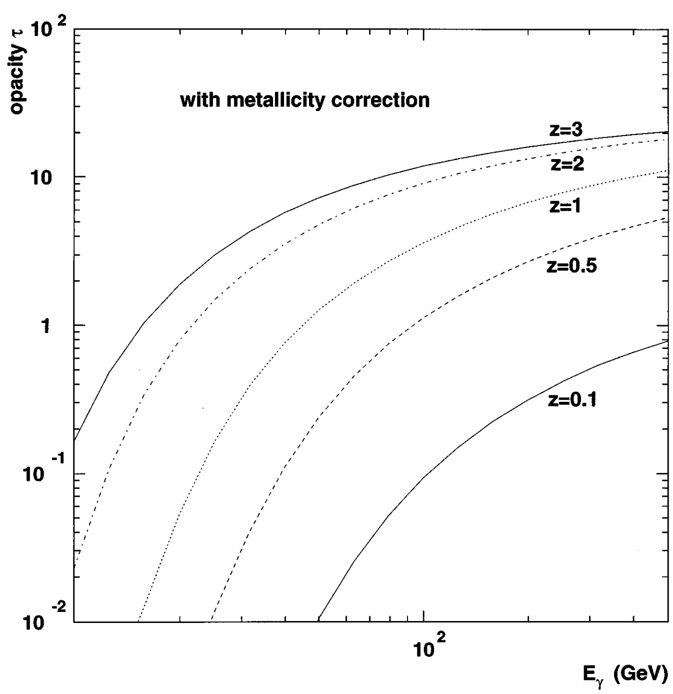

FIG. 6.—Opacity τ of the universal soft photon background to γ-rays as a function of γ-ray energy and source redshift. These curves are calculated with the metallicity correction function included in the expression for stellar emissivity. As discussed in the text, these results are independent of the value chosen for h_0.

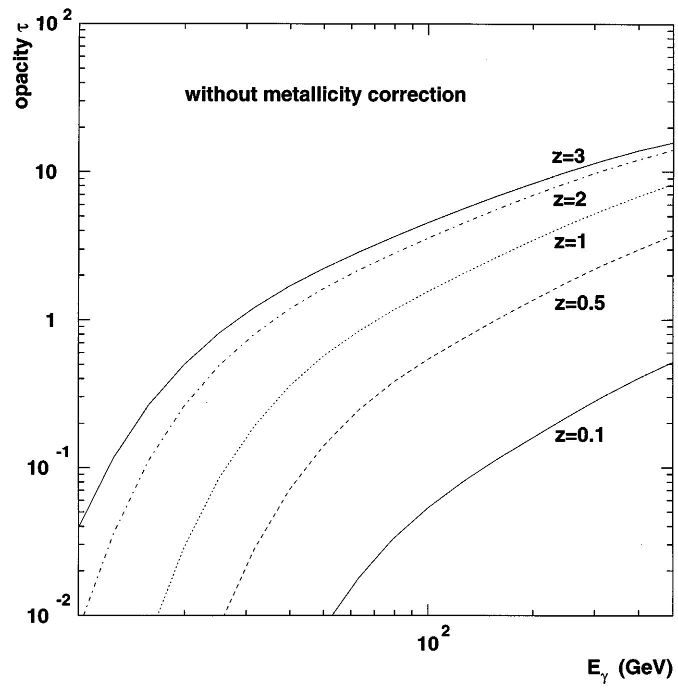

FIG. 7.—Same as Fig. 6, except *without* the metallicity correction function.

The emissivity $\mathscr{E}_\nu$ in equation (4) scales as h_0^2, since neither S_ν, $\mathscr{L}$ nor $dt\dot{\Omega}_*$ depends on h_0, while ρ_c scales as h_0^2. Equation (7) shows then that u_ν scales as h_0, and in equation (10) this h_0 factor is cancelled by the integration over time t.

With the γ-ray opacity $\tau(E_0, z)$ calculated out to $z = 3$, the cutoffs in blazar γ-ray spectra caused by extragalactic pair production interactions with stellar photons can be predicted. Figure 8 shows the effect of the intergalactic radiation background on a few of the γ-ray blazars ("grazars")

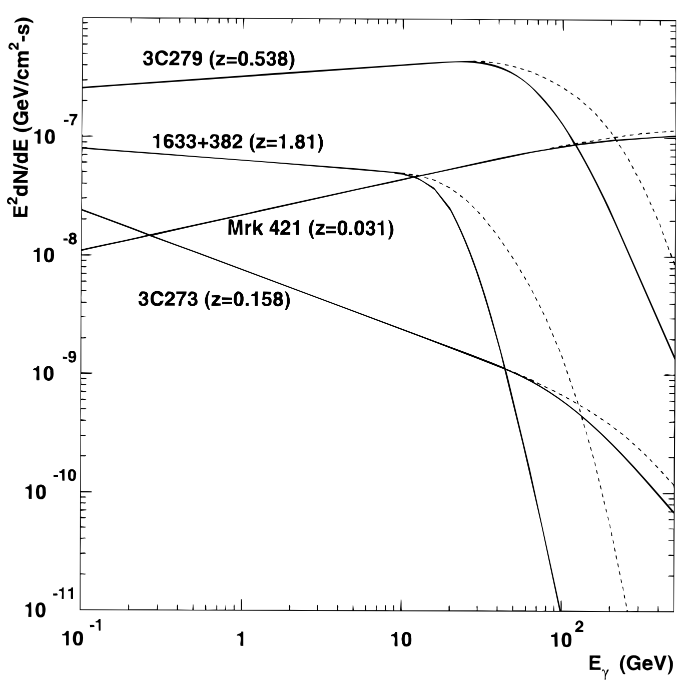

FIG. 8.—Effect of intergalactic absorption by pair production on the power-law spectra of four prominent grazars: 1633+382 ($z = 1.81$), 3C 279 ($z = 0.54$), 3C 273 ($z = 0.15$), and Mrk 421 ($z = 0.031$). The solid (dashed) curves are calculated with (without) the metallicity correction function.

observed by EGRET, viz., 1633+382, 3C 279, 3C 273, and Mrk 421. We have assumed that the mean spectral indices obtained for these sources by EGRET extrapolate out to higher energies attenuated only by intergalactic absorption. Observed cutoffs in grazar spectra may be intrinsic cutoffs in γ-ray production in the source or may be caused by intrinsic γ-ray absorption within the source itself. Whether cutoffs in grazar spectra are primarily caused by intergalactic absorption can be determined by observing whether the grazar cutoff energies have the type of redshift dependence predicted here.

Figure 8 indicates that the next generation of satellite and ground-based γ-ray detectors, both of which will be designed to explore the energy range between 10 and 300 GeV, will be able to reveal information about low-energy radiation produced by galaxies at various redshifts and at different stages in their evolution.

4. CONSTRAINTS ON GAMMA-RAY BURSTS

Our opacity calculations have implications for the determination of the origin of γ-ray bursts, if such bursts are cosmological. As indicated in Figure 6, γ-rays above an energy of ~ 15 GeV will be attenuated if they are emitted at a redshift of ~ 3. On 1994 February 17, the EGRET telescope observed a γ-ray burst that contained a photon of energy ~ 20 GeV (Hurley et al. 1994). If one adopts the opacity results that include our conservative metallicity correction (Fig. 6), the highest energy photon in this burst would be constrained to have most likely originated at a redshift less than ~ 2. (An estimated redshift constraint of ~ 1.5 was given by Stecker & De Jager 1996, based on a simpler model.) Future detectors may be able to place better redshift constraints on bursts observed at higher energies.

5. THE HIGH-ENERGY GAMMA-RAY BACKGROUND FROM BLAZARS

In a previous paper (Stecker & Salamon 1996), we presented a model for calculating the extragalactic γ-ray background (EGRB) due to unresolved grazars. We gave results for γ-ray energies up to 10 GeV (where there is effectively no γ-ray absorption), which were compared to preliminary EGRET data (Kniffen et al. 1996). Using the intergalactic γ-ray opacities calculated here, we can now extend the results of this EGRB model out to an energy of 0.5 TeV.

Our EGRB model assumes that the grazar luminosity function is related to that of flat-spectrum radio quasars (FSRQ), so that we can use FSRQ luminosity and redshift distributions (Dunlop & Peacock 1990) to obtain a grazar luminosity function. The effects of grazar flaring states, γ-ray spectral index variation, and redshift dependence have also been included in this model; see Stecker & Salamon (1996) for details. By integrating the grazar luminosity function weighted by our new opacity results, we obtain a grazar background spectrum up to 500 GeV that properly includes the effect of γ-ray absorption.

Figure 9 shows this EGRB spectrum compared with the preliminary EGRET data. Note that the spectrum is concave at energies below 10 GeV, reflecting the dominance of hard-spectrum grazars at high energies and softer spectrum grazars at low energies; it then steepens above 20 GeV, owing to extragalactic absorption by pair-production interactions with radiation from external galaxies, particularly at high redshifts. Both the concavity and the steepening are signatures of a blazar-dominated γ-ray background spectrum.

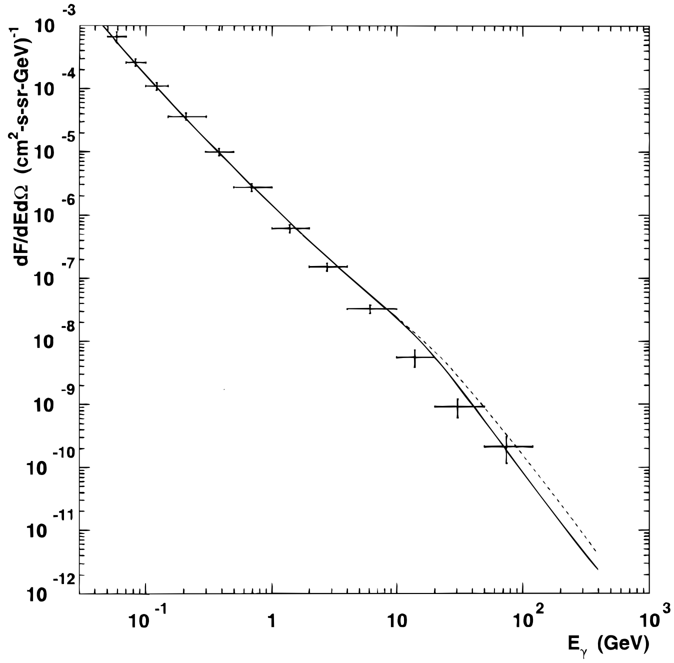

FIG. 9.—Extragalactic γ-ray background energy spectrum from unresolved grazars calculated for a mean EGRET point-source sensitivity of 10^{-7} cm^{-2} s^{-1} for γ-ray energies above 0.1 GeV. Because the FSRQ luminosity function that we employ scales as h_0^3 (Dunlop & Peacock 1990), our calculated EGRB spectrum scales as h_0^2 (see eq. [10] in Stecker & Salamon 1996). The solid (dashed) curves are calculated with (without) the metallicity correction function.

Because the extragalactic γ-ray background in our model is made up of a superposition of lower luminosity, *unresolved* grazars, its intensity is determined by those sources in the universe that are below the detection threshold of a *particular* telescope. A telescope with a superior point-source sensitivity gives a higher source count, thereby reducing the number of unresolved sources that constitute the diffuse γ-ray background. (For a detector more sensitive than EGRET, point-source confusion must also be taken into account in determining this reduction in the background flux.) The EGRB spectrum shown in Figure 9 has been calculated using the mean point-source sensitivity of EGRET above 0.1 GeV, $\sim 10^{-7}$ cm^{-2} s^{-1}. Also shown is the latest analysis of the extragalactic background spectrum obtained by EGRET (Sreekumar et al. 1998).

Above 10 GeV, blazars may have natural cutoffs in their source spectra (Stecker, De Jager, & Salamon 1996), and intrinsic absorption may also be important in some sources (Protheroe & Biermann 1996). Thus, above 10 GeV, our calculated background flux from unresolved blazars, shown in Figure 9, may actually be an upper limit.

6. CONCLUSIONS

We have calculated the γ-ray opacity as a function of both energy and redshift for redshifts as high as $z = 3$ by taking into account the evolution of both the SED and of the emissivity of galaxies with redshift. In order to accomplish this, we have adopted the recent analysis of Fall et al. (1996) and have also included the effects of metallicity evolution on galactic SEDs. We have then considered the effects of the γ-ray opacity of the universe on γ-ray bursts, blazar spectra, and the extragalactic γ-ray background from blazars. In particular, we find that the 1994 February 17 EGRET burst probably originated at $z \leq 2$. Because the stellar emissivity peaks between $z = 1$ and $z = 2$, the γ-ray opacity that we derive shows little increase at higher redshifts. This weak dependence indicates that the opacity is not determined by the initial epoch of galaxy formation, contrary to the speculation of MacMinn & Primack (1996).

The extragalactic γ-ray background, which may be accounted for as a superposition of spectra of unresolved blazars, and which we have predicted to be concave between 0.03 and 10 GeV (Stecker & Salamon 1996), should steepen significantly above 20 GeV owing to our estimates of extragalactic γ-ray absorption at moderate to high redshifts. Both the predicted concavity and steepening may be too subtle to detect with present data from EGRET. However, next generation γ-ray telescopes that are presently being designed, such as *GLAST*, may be able to observe these features and thereby test the blazar background model.

We thank Michael Fall, Matthew Malkan, Yichuan Pei, P. Sreekumar, and Guy Worthey for helpful conversations and comments; P. Sreekumar for making the latest EGRET data on the extragalactic background available before publication; and Ned Wright for alerting us to a significant error in our original manuscript.

REFERENCES

Anderson, R. C., et al. 1979, ApJ, 234, 415
Bertelli, G., et al. 1994, A&AS, 106, 275
Bloom, E. D. 1996, Space Sci. Rev., 75, 109
Bruzual A. G., & Charlot, S. 1993, ApJ, 405, 538
Chandrasekhar, S. 1950, Radiative Transfer (Oxford: Clarendon Press)
Charlot, S., & Bruzual A. G. 1991, ApJ, 457, 625
Charlot, S., Worthey, G., & Bressan, A. 1996, ApJ, 457, 625
Dove, J. B., & Shull, J. M. 1994, ApJ, 430, 222
Dube, R. R., Wickes, W. C., & Wilkinson, D. T. 1979, ApJ, 232, 333
Dunlop, J. S., & Peacock, J. A. 1990, MNRAS, 247, 19
Fall, S. M., Charlot, S., & Pei, Y. C. 1996, ApJ, 464, L43
Fall, S. M., & Pei, Y. C. 1993, ApJ, 402, 479
Gunn, J. E., & Peterson, B. A. 1965, ApJ, 142, 1633
Holberg, J. B. 1986, ApJ, 311, 969
Hurley, K., et al. 1994, Nature, 372, 652
Kniffen, D. A., et al. 1996, A&AS, 120, 615
Lanzetta, K. M., Wolfe, A. M., & Turnshek, D. A. 1995, ApJ, 440, 435
Leitherer, C., Ferguson, H. C., Heckman, T. M., & Lowenthal, J. D. 1995, ApJ, 454, L19
Lilly, S. J., Le Fevre, O., Hammer, F., & Crampton, D. 1996, ApJ, 460, L1
MacMinn, D., & Primack, J. 1996, Space Sci. Rev., 75, 413
Madau, P. 1992, ApJ, 389, L1
———. 1995, ApJ, 441, 18
———. 1997, in AIP Conf. Proc. 393, Star Formation Near and Far, ed. S. S. Holt & L. G. Mundy (New York: AIP), in press
Madau, P., & Meiksin, A. 1994, ApJ, 433, L53
Madau, P., & Phinney, E. S. 1996, ApJ, 456, 124
Madau, P., & Shull, J. M. 1996, ApJ, 457, 551
Madau, P., et al. 1996, MNRAS 283, 1388
Martin, C., Hurwitz, M., & Bowyer, S. 1991, ApJ, 379, 549
Meiksin, A., & Madau, P. 1993, ApJ, 412, 34
Miralda-Escudé, J., & Ostriker, J. P. 1990, ApJ, 350, 1
Paresce, F., McKee, C., & Bowyer, S. 1980, ApJ, 240, 29
Pei, Y. C., & Fall, S. M. 1995, ApJ, 454, 69
Pettini, M., Smith, L. J., Hunstead, R. W., & King, D. L. 1994, ApJ, 426, 79
Protheroe, R., & Biermann, P. L. 1996, Astropart. Phys., 6, 45
Savage, B. D., & Mathis, J. S. 1979, ARA&A, 17, 73
Sreekumar, P., et al. 1998, ApJ, in press
Stecker, F. W. 1996, in AIP Conf. Proc. 348, Unveiling the Cosmic Infrared Background, ed. E. Dwek (New York: AIP), 181
Stecker, F. W., & de Jager, O. C. 1996, Space Sci. Rev., 75, 413
———. 1997 ApJ, 476, 712
Stecker, F. W., De Jager, O. C., & Salamon, M. H. 1992, ApJ, 390, L49
———. 1996, ApJ, 473, L75
Stecker, F. W., & Salamon, M. H. 1996, ApJ, 464, 600
Steidel, C. C., & Sargent, W. L. W. 1987, ApJ, 318, L11
Tennyson, P. D., Henry, R. C., Feldman, P. D., & Hartig, G. F. 1988, ApJ, 330, 435
Thompson, D., et al. 1996, ApJS, 107, 227
Toller, G. N. 1983, ApJ, 266, L79
Vogel, S. N., Weymann, R. J., Rauch, M., & Hamilton, T. 1995, ApJ 441, 162
Whittet, D. C. B. 1992, Dust in the Galactic Environment (Bristol: IOP)
Wolfe, A. M. 1986, Philos. Trans. R. Soc. London, A, 320, 503
Worthey, G. 1994, ApJS, 95, 107